# Heat and Mass Transfer of Thermophoretic Magneto-Micropolar Fluid Passing an Inclined Plate with Chemical Reaction in Porous Medium

**Fatunmbi E. O. *[1], Agbolade A. O. [2]**
Department of Mathematics and Statistics, Federal Polytechnic, Ilaro, Nigeria
*Corresponding author: olusojiephesus@yahoo.com: +2348034013598

**ABSTRACT**

Transfer of heat and mass in a reactive electrically conducting fluid of micropolar type being impacted with thermophoresis is the focus of this research. The problem is on two-dimensional geometry and taken to be steady, viscous flow being influenced by buoyancy force, varying heat production, absorption as well as dissipating effects. The formulated model equations are simplified via the approach of similarity conversion analysis while the solutions are gotten numerically by means of Runge-Kutta-Fehlberg integration algorithm in company of shooting techniques. Various graphs are sketched and tables constructed to discuss the impact of some of the controlling quantities on the flow, thermal and solutal fields. A strong relationship exists between the solution obtained with existing related ones in literature in some limiting situations. It is observed from the results that the fatness of the momentum and concentration boundary layers is lower in a thermophoretic as well as reactive fluids while thermal conductivity term offers an opposite trend.

**Keywords**: Micropolar fluid; inclined sheet; porous medium; Thermophoresis

## INTRODUCTION

The study of combined heat and mass transfer is prominent in science, engineering and manufacturing activities for instance in designing and building relevant equipment, gas turbines, satellites and space vehicles, nuclear plants, electric transformers, etc. The occurrence of transport phenomenon is encountered both in nature and industrial works due to heat and mass transfer influence happening simultaneously in viwe of combined buoyancy influences.. These processes can be encountered in food processing, storage operations in agricultural processes, polymer production and diverse chemical industries. (Pal and Chatterjee, 2010, Mohapatra, Pattanayak and Mishra, 2015; Mishra, Baag and Mohapatra, 2016; Reddy and Chamkha, 2016)).

Fluid flow passing porous media has become crucial in different areas of science and technology due to its various relevance such as in spreading of chemical pollutants in saturated soil, crude oil extraction, ground water hydrology, irrigation systems and in biomedical engineering such as, drug delivery and tissue implant. To this end, Rahman and Sultana (2008) obtained local similarity solutions numerically on flow fluid in MHD micropolar type in a porous medium and noted that the skin friction coefficient is a decreasing function of Darcy parameter. Olajuwon, Oahimire and Waheed (2014) applied perturbation method to study such problem and showed that both Darcy and inertia parameters caused a decline in the locomotion. Kumar (2017) investigated such problem when the sheet is inclined with isothermal boundary heating and chemical reaction of order one. The applications of the study with chemical reactions and heat generation/absorption in hydrometallurgical companies as well as chemical processing factories are important. These include food processing, drying processes, groves of fruit trees and crop damage due to freezing. Motivated by these, Mohamed and Abo-Dahab (2009) numerically addressed the influence of homogeneous order one reaction with the impact of radiation in MHD micropolar flow passing a vertical surface in a porous medium being impacted with production of heat. Besides, Mishra *et al.* (2016) obtained numerical solution for such problem being influenced by thermo-diffusion along an impermeable stretching sheet.

The thermophoresis concept is a phenomenon that can occur when the force of temperature gradient act on the mixtures of mobile particles such that the various particles display different reactions to that force. In order words, this phenomenon relates to the movement of colloidal particles due to macroscopic temperature. The occurrence of temperature gradient in gas influences the various particles suspended in the gas to migrate in the direction of declining temperature. The most common example of this is seen during the blackening of the glass globe of a lantern using kerosene. In such scenario, the temperature gradient occurring between the flame and the globe forces the carbon particles created during the combustion activities to settle down on the globe (see

Talbot, Cheng, Scheffer and Wills, 1980; Animasaun, 2015). The application of this concept includes aerosol collection, micro contamination control, nuclear reactor safety, in determining exhaust gas particle trajectories from combustion devices and many more (see Animasaun, 2015; Parida, Panda and Rout, 2015). This kind of study was first reported by Goldsmith and May (1966) who investigated the occurrence of thermophoretic transport concept with the assumption of simple one-dimensional flow. Thereafter, various investigators (see Aurangzaib and Shafie, 2012; Jyothi, Sreelakshmi, Nagendramma and Sarojamma, 2015; Das, Jana and Kundu, 2015; Animasaun, 2015; Mondal, Dulal, Sewli, Chatterjee, Precious Sibanda a *et al.*, 2017) have considered this subject using various geometries, diverse parameters and methods. None of these researchers however considered the use of non-Newtonian micropolar fluid as the working fluid inspite of its huge applications.

Researches on boundary layer flow with impact of heat transfer characteristics involving the fluid of Newtonian type have been considered over the years. However, scientists and researchers have on the recent times focused much on the studies of non-Newtonian in view of its practical applications both industrially and in engineering operations. Notable among the various concepts of non-Newtonian fluids is the micropolar fluid. The concept of this fluid concerns fluids with microstructures and rigid spherical bar-like parcels. Due to inherent microstructural characteristics of these fluids, they offer good mathematical framework in modelling and simulating complex and complicated fluids which cannot be effectively captured by the Navier-Stokes model (Newtonian model). Examples are: polymeric, suspensions fluids, animal blood, lubricants, liquid crystals, colloidal fluids and so on (Qasim, Khan and Shafle, 2013; Srinivasacharya and Mendu, 2014).

The theory of micropolar fluid as well as that of thermal micropolar fluid was pioneered by Eringen (1966, 1972). This model enables the coupling of microrotation and macro-velocity fields thereby displaying some microscopic effect leading to both translation and rotation of the fluid element. There is a wide applications of such fluids in engineering and industrial operations for instance, in the bio-mechanic and chemical engineering, extrusion of polymer, slurry technologies, synovial lubrication, arterial blood flows, knee cap mechanics, a few of many (Lukaszewicz, 1999; Reena and Rana, 2009). Moreso, investigations of heat and mass transfer over various configurations engaging micropolar fluid have possible applications in biomedical and engineering activities such as in the dialysis of blood in artificial kidney, blood flows, fluid flow in brain, flow in oxygenation, porous pipe design, design of filter (Reena and Rana, 2009; Olajuwon êt al., 2014). In view of these usefulness, several authors (see Mohamed and Abo-Dahab, 2009; Pal and Chatterjee, 2010; Olanrewaju, Adeniyan and Alao, 2013; Mishra *et al.*, 2016; Kumar, 2017; Salawu and Fatunmbi, 2016; Fatunmbi and Fenuga, 2017) have investigated such studies with various parameters of interest, boundary conditions and methods. However, in all these studies, the effect of thermophoresis have been ignored by the researchers.

In particular, the immense applications of studies on heat and mass transfer influenced by thermophoresis and chemical reaction have propelled the setting of this study. This research work is therefore set out to numerically investigate thermophoretic flow of an electrically conducting non-Newtonian micropolar fluid passing an inclined sheet in a porous medium under the influence of viscous dissipation and non-uniform heat source/sink. The possible applications of this study can be found in the biomedical engineering such as drug delivery and tissue implant and other areas of engineering including crude oil extraction, ground water hydrology, irrigation system, etc. In the absence of microrotation vector, vortex viscosity and spin gradient viscosity, this study coincides with that of Mondal *et al.* (2017). Hence, the comparison of the computed values of some physical parameters relating to the skin friction coefficient and Nusselt number with that of Mondal *et al.*, (2017) and Alam *et al.* (2006) in the limiting situations.

## Mathematical Analysis and Formulation of the Model

Considering a convective steady flow of micropolar fluid on a two-dimensional, semi-infinite permeable inclined sheet in a porous medium as showcased in Fig. 1. The sheet is inclined at an angle $\varphi$ to the vertical, the $x$ axis is the coordinate measured along the sheet with $y$ axis perpendicular to it, a magnetic field of strength $B_0$ is imposed perpendicular to the flow direction while the induced magnetic field is ignored on the account of low magnetic Reynolds number, a uniform suction is also imposed at the sheet surface. The model includes homogeneous order one chemical reaction impact as well as thermophoresis (see equation 7-8) . The flow with transfer of heat is being influenced by varying heat source/sink (see equation 6) and viscous dissipation effect while the fluid properties have been assumed to be uniform in nature apart from the density variation in buoyancy terms found in equation (2) which is approximated via Boussinesq approximation.

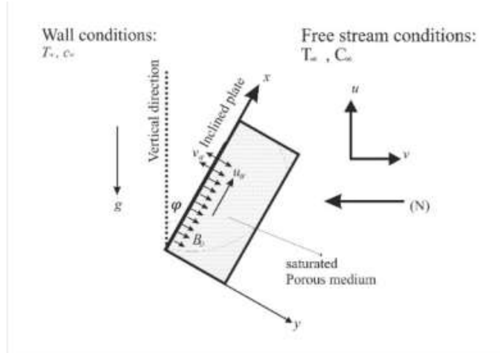


**Fig.1** The Geometry of the Physical Model

Bearing in mind the aforementioned suppositions together with boundary layer approximation, the derived governing equations are presented below:

$$\frac{\partial u}{\partial x}+\frac{\partial v}{\partial y}=0, \tag{1}$$

$$u\frac{\partial u}{\partial x}+v\frac{\partial u}{\partial y}=\left(\frac{\mu+\mu_r}{\rho}\right)\frac{\partial^2 u}{\partial y^2}+\frac{\mu_r}{\rho}\frac{\partial \omega}{\partial y}+g\beta_T(T-T_\infty)cos\varphi+g\beta_C(C-C_\infty)cos\varphi-\frac{\sigma B_0^2}{\rho}u-\frac{\mu}{\rho k_p}u \tag{2}$$

$$u\frac{\partial \omega}{\partial x}+v\frac{\partial \omega}{\partial y}=\frac{\gamma}{\rho j}\frac{\partial^2 \omega}{\partial y^2}-\frac{\mu_r}{\rho j}\left(2\omega+\frac{\partial u}{\partial y}\right) \tag{3}$$

$$u\frac{\partial T}{\partial x}+v\frac{\partial T}{\partial y}=\frac{\kappa}{\rho c_p}\frac{\partial^2 T}{\partial y^2}+\frac{(\mu+\mu_r)}{\rho c_p}\left(\frac{\partial u}{\partial y}\right)^2+\frac{\sigma B^2}{\rho c_p}u^2+\frac{\mu}{\rho c_p k_p}u^2+\frac{q'''}{\rho c_p}+\frac{DmK_T}{CsC_p}\frac{\partial^2 C}{\partial \bar{y}^2}, \tag{4}$$

$$u\frac{\partial C}{\partial \bar{y}}+v\frac{\partial C}{\partial y}=Dm\frac{\partial^2 C}{\partial y^2}+\frac{DmK_T}{T_m}\frac{\partial^2 T}{\partial y^2}-k_r(C-C_\infty)-\frac{\partial}{\partial y}(V_T C) \tag{5}$$

Where $q'''$ in equation (4) is presented as (see Olajuwon *et al.* 2013; Pal and Mondal, 2014 and Das *et al.*, 2015)

$$q'''=\frac{\kappa U_0}{2xv}[(T_w-T_\infty)(\alpha e^{-\eta}+\beta\theta)], \tag{6}$$

The thermophoretic velocity $V_T$ in equation (5) is written as

$$V_T=-\frac{k_t^\star}{T_{ref}}\frac{\partial T}{\partial y}, \tag{7}$$

and the thermophoresis coefficient $k_t^\star$ is defined to be

(8)

The associated conditions at the boundary are:

$$u=U_0, v=V_w, \omega=-r\frac{\partial u}{\partial y}, T=T_w, C=C_w at y=0,$$
$$u=0, \omega\longrightarrow 0, T\longrightarrow T_\infty, C\longrightarrow C_\infty as y\rightarrow\infty. \tag{9}$$

From the governing equations (1-5), $u$ and $v$ describe the velocity components along $x$ and $y$ axis in that order, $\mu$ stands for dynamic viscosity while $\nu$ denotes kinematic viscosity with $\kappa$ symbolizing thermal conductivity, $\rho$ denotes density of the fluid whereas the vortex viscosity is denoted by $\mu_r$ while $j$ symbolizes micro-inertial density, $c_p$ symbolizes specific heat at constant pressure and $\gamma$ connotes the spin gradient viscosity. Similarly, $T, T_w, T_\infty$ and $\omega$ correspond to fluid temperature, sheet and free stream temperatures, microrotation component in that order. The suction/injection term is denoted by $V_w$, $\sigma$ is the electrical conductivity while $\beta_T, \beta_C, k_r$, $k_p, Dm, Cs$ and $T_m$ describe coefficient of thermal expansion, coefficient of solutal expansion, chemical rate of reaction, porous medium permeability, mass diffusivity, fluid susceptibility and mean fluid temperature in that order.

Meanwhile, $\alpha$ and $\beta$ symbolize space and heat dependent source/sink respectively, $C_1, C_2, C_3, C_m$ and $C_t$ are constants while $k_s$ represents the diffused particles thermal conductivity whereas $K_n$ is the Knudsen number. Typical value of $\tau$ are 0.01, 0.05 and 0.1 relating to the approximate values of $-k_t^\star(T_w-T_\infty)$ equivalent to

$3K, 15K$ and $30K$ for $T_{ref} = 300K$. The parameter $r$ in equation (9) stands for micropolar surface concentration parameter such that $0 \leq r \leq 1$. For the case $r = 0$, then $\omega = 0$ as described by Jena and Mathur (1981), it is a condition of strong concentration of the micro-particles at the wall where the micro-particles close the wall are incapable of rotation or translation. Meanwhile, Ahmadi (1976) discussed a situation of weak concentration such that effect of the microstructure is negligible in the neighbourhood of the boundary, in this case, is relevant. However, $r = 1$ is applicable for turbulent boundary layer situations as opined by Peddieson (1972). The level at which micropolar fluid deviates from the classical Newtonian fluid concept can be discovered by the size of parameter $\mu_r$, thus, when $\mu_r = 0$, then equations (2) and (4) are decoupled from equation (3). Then the model addressed in this study as well as the results obtained corresponds to that of Newtonian fluid model. We have also assumed that $V_w = V_0 x^{-1}$, $\sigma = \sigma_0 x^{-1}, \beta_T = \beta_0 x^{-1}, \beta_C = \beta_0^{\star} x^{-1}, k_r = k_1 x^{-1}, k_p = k_0 x$ where $V_0, \sigma_0, \beta_0, \beta_0^{\star}, k_1$ and $k_0$ are constants (Ishak, 2010;, Makinde, 2012, Parida *et. al.*, 2015).In line with previous authors (Rahman, Aziz and Al-Lawatia, 2012; Mondal *et al.*, 2017), the underlisted similarity variables (10) are used to transmute the model equations

(10)

The use of quantities (10) ensures the validity of equation (1). Taking cognizance of equations (6-8) and using (10) equations (2-5) translate to:

$$(1+K)f''' + Kg' + ff'' + Gr\theta\cos\varphi + Gc\phi\cos\varphi - [Da + M]f' = 0, \tag{11}$$

(12)

$$\theta'' + Prf\theta' + (1+K)PrEcf''^2 + PrEc(M + Da)f'^2 + (\alpha e^{-\eta} + \beta\theta) + PrDu\phi'' = 0. \tag{13}$$

$$\phi'' + Sc(f - \tau\theta')\phi' - Sc\zeta\phi + Sc(Sr - \tau\phi)\theta'' = 0, \tag{14}$$

the conditions at the boundary also become

$$\begin{gathered} f'(0) = 1, f(0) = fw, g(0) = -rf'', \theta(0) = 1, \phi(0) = 1 \\ f'(\infty) = 0 g(\infty) = 0, \theta(\infty) = 0, \phi(\infty) = 0. \end{gathered} \tag{15}$$

The description of the symbols used in Eqs. (11-15) are expressed below

$$\begin{gathered} fw = \frac{-\sqrt{2}V_0}{(\sqrt{U_0 \nu})}, M = \frac{2\sigma_0 B_0^2}{\rho U_0}, Gr = \frac{2g\beta_0(T_w - T_\infty)}{U_0^2}, Gc = \frac{2g\beta_0^{\star}(C_w - C_\infty)}{U_0^2}, \\ K = \frac{\mu_r}{\mu}, Ec = \frac{U_0^2}{cp(T_w - T_\infty)}, Pr = \frac{\mu c_p}{\kappa}, Da = \frac{2\nu}{k_o U_0}, Sc = \frac{\nu}{Dm}, \zeta = \frac{2k_1}{U_0} \\ Du = \frac{DmK_T}{CsCp\nu}\left(\frac{C_w - C_\infty}{T_w - T_\infty}\right), Sr = \frac{DmK_T}{Tm\nu}\left(\frac{T_w - T_\infty}{C_w - C_\infty}\right), \tau = -\frac{k_t^{\star}(T_w - T_\infty)}{T_{ref}}. \end{gathered} \tag{16}$$

In equation (16) the material parameter is indicated by $K$, the suction/injection parameter is symbolized as $fw$ with $fw > 0$ indicating suction while $fw < 0$ relates to injection whereas an impermeable sheet is described when $fw = 0$. Moreso, $M$ depicts the magnetic field term while the thermal Grashof number is indicated by $Gr$, the solutal Grashof number is symbolized by $Gc$, $Pr$ is the Prandtl number, $Du$ symbolizes Dufour number, $Sr$ indicates Soret number, $\zeta$ connotes chemical reaction rate, Eckert number is represented as $Ec$ while differentiation is carried out with respect to $\eta$ and $\tau$ is the thermophoretic term.For engineering purposes, the relevant quantities are the skin friction coefficient, Nusselt and Sherwood numbers which are orderly presented in equation (17).

$$C_{fx} = \frac{\tau_w}{\rho u_w^2}, Nu_x = \frac{xq_w}{\kappa(T_w - T_\infty)}, Sh_x = \frac{xq_m}{Dm(C_w - C_\infty)}, \tag{17}$$

with $\tau_w$ being shear stress, $q_w$ heat flux at the surface and $q_m$ is the mass flux at the surface such that

$$\tau_w = \left[(\mu + \mu_r)\frac{\partial u}{\partial y} + \mu_r N\right]_{y=0}, q_w = -\left[\kappa\frac{\partial T}{\partial y}\right]_{y=0}, q_m = -\left[Dm\frac{\partial C}{\partial y}\right]_{y=0} \tag{18}$$

upon substituting (10) and (18) in (17), the skin friction coefficient yields

(19)

while the Nusselt and Sherwood numbers respectively transform to

. (20)

**SOLUTION METHOD**

The set of equations (11-14) together with the wall conditions (15) constitute a highly nonlinear equations which the closed form analytical solution is not feasible. Hence, in this study, numerical solution has been sought via shooting technique in company with Runge-Kutta-Fehlberg integration. By this approach, an appropriate finite value of $\eta \rightarrow$ has been chosen (say $\eta_\infty$) and the set of governing equations (11-14) is translated into a system of nine first order simultaneous linear equations and thereafter reduced into an initial value problem (IVP) by means of shooting method. However, to solve this set of equations as an IVP requires nine initial conditions for the solution but only five are available. To start the process of solution therefore, some initial guess are selected for the unknown initial conditions $h_1, h_2, h_3$ and $h_4$ to obtain $f''(0), g'(0), \theta'(0)$ and $\phi'(0)$. This process is repeated with a larger $\eta_\infty$ and continues until the solution for which successive values of the unknown initial conditions $f''(0), g'(0), \theta'(0)$ and $\phi'(0)$ gives a difference after a intended significant digit. The end value of $\eta_\infty$ is then selected as siutable value of the limit $\eta_\infty$ for a particular set of controlling quantities. Let

$$r_1 = f, r_2 = f', r_3 = f'', r_4 = g, r_5 = g', r_6 = \theta, r_7 = \theta', r_8 = \phi, r_9 = \phi', \tag{21}$$

$$r_3{}' = -\left[\frac{Kr_5 + r_1 r_3 + Grr_6 cos\varphi + Gcr_8\varphi + (Da+M)r_2}{(1+K)}\right], \tag{22}$$

(23)

$$r_7{}' = -[Prr_1r_7 + (1+K)PrEcr_3 + PrEc(M+Da)r_2 + (\alpha e^{-\eta} + \beta r_6) + PrDur_9{}'], \tag{24}$$

$$r_9{}' = Sc\zeta r_8 - Sc(Sr - \tau r_8)r_7{}' - Sc(r_1 - \tau r_7)r_8, \tag{25}$$

with the boundary conditions given as

$$\begin{gathered} r_1(0) = 0, r_2(0) = 1, r_3(0) = h_1, r_4(0) = -rf_3(0), r_5(0) = h_2, r_6(0) = 1, r_7(0) = h_3, \\ r_8(0) = 1, r_9(0) = h_4, r_2(\infty) \rightarrow 0, r_4(\infty) \rightarrow 0, r_6(\infty) =\rightarrow 0, r_8(\infty) =\rightarrow 0. \end{gathered} \tag{26}$$

When all the initial conditions are obtained, then Runge-Kutta-Fehlberg integration scheme engaged to solve the resulting set of equations simultaneously using Maple 2016.

RESULTS ANALYSIS AND DISCUSSION

The behaviour of emerging parameters listed in (16) on the velocity, temperature, concentration as well as on the quantities of engineering concern are analyzed in this section using tables and graphs. The validity of the numerical code has been verified by comparing the results obtained in this study relating to $C_{f_x}$ and $Nu_x$ with those reported by Alam, Ferdows, Ota, Maleque (2006) and Mondal *et al.* (2017) in the absence of $K, \tau, \alpha, \beta, \zeta, \varphi, Ec$ and $Da$. These values are recorded in Table 1 and found to be in excellent relationship. The computational values used for the analysis in this study have been carefully selected from previous researchers, these are: unless stated otherwise on various plots.

**Table 1:** Computed values of $C_{f_x}$ and $Nu_x$ for changes in $Du$ and $Sr$

| $Du$ | $Sr$ | Alam *et al.* | | Mondal *et al* | | Present study | |
|---|---|---|---|---|---|---|---|
| | | $C_{fx}$ | $Nu_x$ | $C_{fx}$ | $Nu_x$ | $C_{fx}$ | $Nu_x$ |
| 0.03 | 2.0 | 6.2285 | 1.1565 | 6.238707 | 1.151932 | 6.229908 | 1.156453 |
| .037 | 1.6 | 6.1491 | 1.1501 | 6.160867 | 1.144651 | 6.150610 | 1.150059 |
| .050 | 1.2 | 6.0720 | 1.1428 | 6.087934 | 1.135752 | 6.073556 | 1.142710 |
| .075 | 0.8 | 6.0006 | 1.1333 | 6.023187 | 1.123219 | 6.002251 | 1.133220 |
| .150 | 0.4 | 5.9553 | 1.1157 | 5.996934 | 1.096560 | 5.957028 | 1.115613 |

The variation of material term $K$ on the flow, temperature and microrotation fields in the presence of different values of the magnetic field parameter is plotted in Figures 2a, 2b and 3a. The velocity reaches the maximum (Figure 2a) and decreases near the sheet with a rise in $K$ whereas away from the inclined sheet at $\eta \approx 1.5$, the profiles intersect and the trend is reversed with a rise in fluid locomotion due a fall in the dynamic viscosity as

$K$grows. An increase in the magnetic field term $M$ leads to a fall in the velocity as seen in this figure. This in respect of Lorentz force created by the imposition of the transverse magnetic field to the electrically conducting micropolar fluid, as $M$ therefore rises, the fluid motion is resisted and lowered. Due to the resistance to the fluid flow produced by the Lorentz force as $M$ grows, the temperature distribution is boosted as portrayed in Figure 2b. In the like manner, the temperature is found to appreciate with rising values of the micropolar fluid $K$. The microrotation profile rises with growing values of both $K$ and $M$ as shown in Figure 3a with a reverse rotation of the micro-particles occurs with an increase in the value of $K$. The influence of $Gr$ is to enhance the motion of the fluid as depicted in Figure 3b.

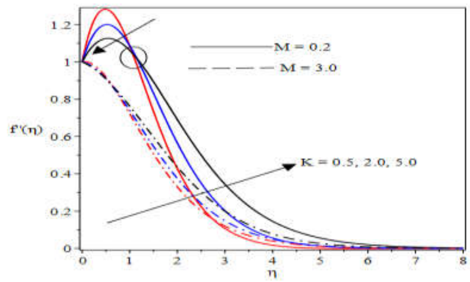


**Figure 2a**

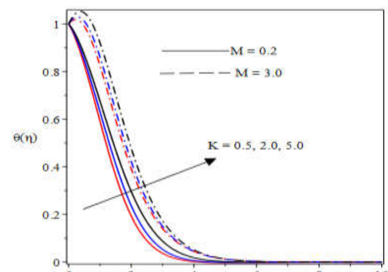


**Figure 2b**

**Figure 2:** Variation of material (micropolar) $K$ and magnetic field $M$ parameters on (a) velocity field and (b) temperature field.

Physically, $Gr$ describes the relative influence of thermal buoyancy to the viscous force, hence, growing values of $Gr$ acts as a suitable pressure gradient causing the fluid motion to rise. Conversely, increasing values of Darcy term $Da$ enhances the tightness of the porous medium thereby lowering the fluid locomotion as displayed in Figure 3b.

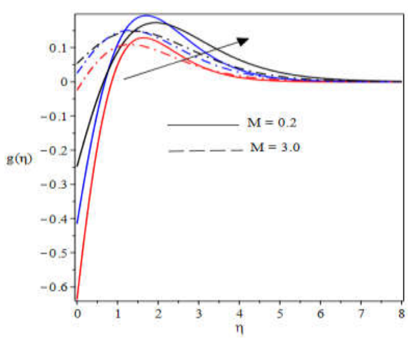


**Figure 3a**

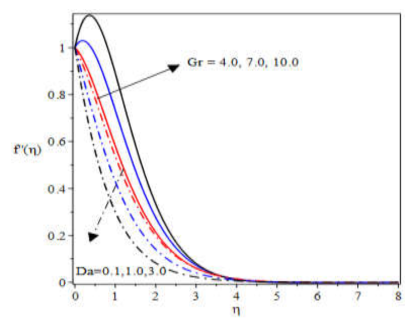


**Figure 3b**

**Figure 3:** (a) The impact of material $K$ and magnetic field $M$ parameters on microrotation profiles and (b) effect of thermal Grashof $Gr$ and Darcy parameters $Da$ on velocity profiles.

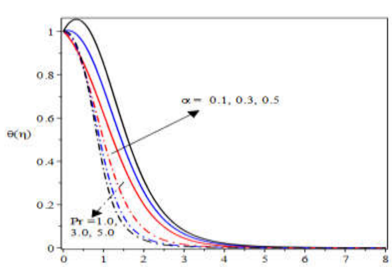


**Figure 4a**

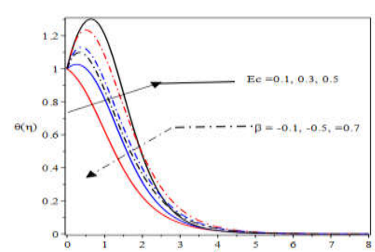


**Figure 4b**

**Figure 4:** Reaction of temperaturefield to variation in (a) Prandtl number $Pr\&\alpha > 0$ (b) Eckert number $Ec\&\beta < 0$

Figure 4a reveals the response of the thermal field to varying values of Prandtl number $Pr$ and space heat generation term $\alpha > 0$. The Prandtl number $Pr$ describes the rate at which thermal diffusion occurs as compared with momentum diffusion, an increase in $Pr$ creates thinning boundary layer effect and consequently lower the temperature distribution.

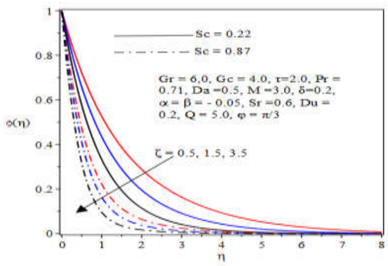


**Figure 5**

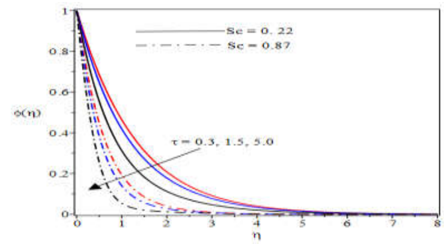


**Figure 5b**

**Figure 5:** Concentration distribution for various of (a) chemical reaction $\zeta$& Schmidt $Sc$ parameters (b) thermophoresis $\tau$& Schmidt $Sc$ parameters.

Moreso, in Figure 4a, the temperature is seen to advance with rising values of $\alpha$ owing to the fact that a rise in $\alpha$ leads to production of more heat thereby causing the micropolar fluid temperature to escalate. Figure 4b is a graph of the temperature against $\eta$ for varying values of Eckert number $Ec$ and heat absorption term $\beta < 0$. Growing values of $Ec$ encourages the growth of temperature owing to additional heat generated by the frictional drag of the fluid particles whereas the opposite is the case for the heat absorption parameter $\beta < 0$ due to a decline in the thickness of the thermal boundary layer with a growth in the heat absorption term.

Figure 5a describes the graph of the concentration field versus $\eta$ for changes that occur in the term indicating chemical reaction $\zeta$ in the presence of the Schmidt number $Sc$.It is found that increasing values of both $\zeta$ and $Sc$ lead to a fall in the concentration field. The thinning of the boundary layer structure is discovered for growth in both terms. In the same vein, Figure 5b demonstrates that the influence of the thermophoresis term $\tau$ is to dampen the structure of the boundary layer and consequently lower the concentration filed.

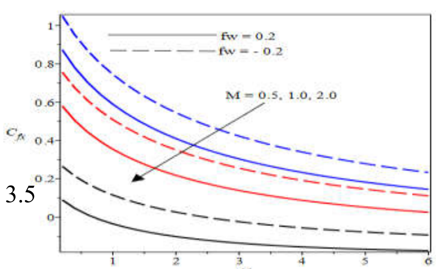


**Figure 6a**

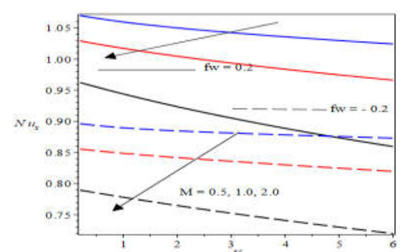


**Figure 6b**

**Figure 6:** Combined impact of micro[olar parameter $K$ and magnetic field parameter $M$ on (a) $C_{fx}$ and (b) $Nu_x$

It is evident in Figure 6a that the effects of both $M$ and $K$ are to reduce the skin friction coefficient $C_{fx}$ in the presence of both suction and injection terms, however, $C_{fx}$ is better reduced in the presence of suction as noticed in this case. In the same manner, the response of the Nusselt number as observed in Figure 6b is similar to that of $C_{fx}$ that is, $Nu_x$ reduces but the heat transfer is lower for injection $fw < 0$ in this situation. From these plots, it is remarked that suction/injection is applicable in stabilizing the boundary layer growth.

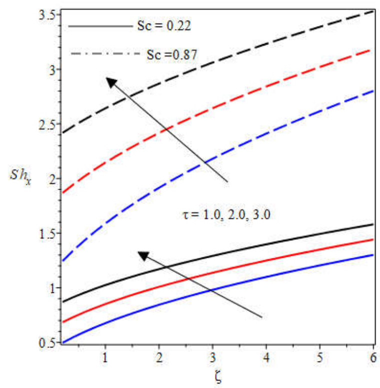


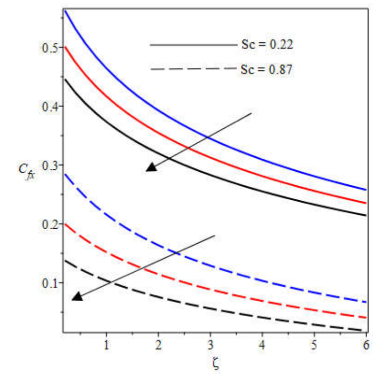


**Figure 7a** **Figure 7b**

**Figure 7:** Combined influence of chemical raection parameter $\zeta$ and thermophoresis parameter $\tau$ on (a) Sherwood number and (b) skin friction coefficient $C_{fx}$.

'Figures 7a and 7b describe the plots of the Sherwood number against $\zeta$ for variation in the thermophoresis parameter $\tau$ in the presence of Schmidt number $Sc$. It is revealed that the mass transfer is boosted by increasing thermophoresis term $\tau$, likewise, for any chosen value of $\tau$ an increase $\zeta$ also causes $Sh_x$ to appreciate. However, in these cases, the increase in $Sh_x$ is higher for heavier molecules as noticed in Figure 7a. Increasing values of $\tau$ creates a reducing influence on $C_{fx}$ as depicted in Figure 7b, in the like manner, an increase in $\zeta$ for any fixed value of $\tau$ also lowers $C_{fx}$.

CONCLUSION

This research work has theoretically investigated the flow, heat and mass transfer of thermophoretic magneto-micropolar reactive fluid moving in an inclined two-dimensional sheet influenced by non-uniform heat source/sink, buoyancy forces, viscous dissipation as well as Soret-Dufour effects. The modelled equations governing the flow, heat and mass transfer have been solved numerically by means of shooting technique in company of Runge-Kutta-Fehlberg scheme. Comparison of the presented work with existing results in literature as special cases of the current study assures good agreement. We have constructed various graphs to illustrate the impact of the main controlling parameters in this study. From this study, the following points were deduced.

- The fluid flow is lowered with imposition of the magnetic field $M$ and Darcy $Da$ parameters whereas it rises with rising values of the buoyancy force $Gr$ and material (micropolar) $K$ parameters.
- The mass transfer appreciates with growing values of the thermophoresis parameter $\tau$ and Schmidt number $Sc$ whereas both parameters act to $C_{fx}$.
- The presence of the microstructure particles and the magnetic field term facilitate the fall in the viscous drag stress $C_{fx}$ and the heat transfer rate $Nu_x$ across the boundary layer.
- An increase in $Ec, \alpha, M$ and $K$ lead to the thickening of the thermal boundary layer thickness whereas the opposite occurs when the magnitude of $Pr$ and $\beta < 0$ rise.
- The growing values of the chemical reaction $\zeta$, Schmidt number $Sc$ and thermophoresis parameters $\tau$ tend to reduce the thickness of the concentration boundary layer and consequently lower the concentration distribution across the boundary layer.

**REFERENCES**


Ahmadi, G. (1976). Self-similar solution of incompressible micropolar boundary layer flow over a semi-infinite plate. *Int. J. Engng. Sci, 14*, 639-646.

Animasaun, I. L. (2015). Effects of thermophoresis, variable viscosity and thermal conductivity on free convective heat and mass transfer of non-darcian MHD dissipative Casson fluid flow with suction and nth order of chemical reaction. *Journal of Nigerian Mathematical Society, 34*, 11-31.

Alam, M. S, Ferdows, M., Ota, M., Maleque, M. A. (2008). Dufour and Soret effects on steady free convection and mass transfer flow past a semi-infinite vertical porous plate in a porous medium. *Int J Appl Mech Eng, 11*(3):535-545.

Aurangzaib, Md., Uddin, S., Bhattacharyya, K. and Shafie, S. (2016). Micropolar fluid flow and heat transfer over an exponentially permeable shrinking sheet, *Propulsion and Power*, 1-8.

Das, K. and Jana, S. and Kundu, P.K. (2015), Thermophoretic MHD Slip Flow over a permeable surface with variable fluid properties. *Alexandria Engineering Journal*, 35- 44.

Eringen, A. C. (1966). Theory of micropolar fluids. *J. Math. Anal. Appl., 16*, 1-18.

Fatunmbi, E. O. and Fenuga, O. J. (2017). MHD micropolar fluid flow over a permeable stretching sheet in the presence of variable viscosity and thermal conductivity with Soret and Dufour effects. *International Journal of Mathematical Analysis and Optimization: Theory and Applications, 2017*, 211- 232.

Ishak, A. (2010). Similarity solutions for flow and heat transfer over a permeable surface with convective boundary condition, *Applied Mathematics and Computation, 217*, 837-842.

Goldsmith, P and May, F. G. (1966). *Diffusiophoresis and thermophoresis in water vapour systems, in: Aerosol Science*, Academic Press, London.

Jena, S. K. and Mathur, M. N. (1981). Similarity solutions for laminar free convection flow of a thermomicropolar fluid past a non-isothermal flat plate. *Int. J. Eng. Sci. 19*, 1431-1439.

Jana, S. and Das, K. (2015). Influence of variable fluid properties, thermal radiation and chemical reaction on MHD flow over a flat plate. *Italian Journal of Pure and Applied Mathematics*, 34, 20-44.

Kumar, H. (2017). Heat and mass transfer on isothermal inclined porous plate in the presence of chemical reaction. *International Journal of Pure and Applied Mathematics, 113*(5), 523-539. Doi: 10.12732/ijpam.v113i5.1

Lukaszewicz, G. (1999). *Micropolar fluids: Theory and Applications* (1st Ed.). Birkhauser, Boston.

Makinde, O. D., Khan, W. A., Culham, J. R. (2016). MHD variable viscosity reacting flow over a convectively heated plate in a porous medium with thermophoresis and radiative heat transfer. *International Journal of Heat and Mass Transfer, 93*, 595-604.

Mondal, H., Pal, D., Chatterjee, S. and Sibanda, P. (2017). Thermophoresis and Soret-Dufour on MHD mixed convection mass transfer over an inclined plate with non-uniform heat source/sink and chemical reaction. *Ain Shams Engineering Journal, 2017*, 1-11.

Mishra, S. R, Baag, S. and Mohapatra, D. K. (2016). Chemical reaction and Soret effects on hydro magnetic micropolar fluid along a stretching sheet, *Engineering Science and Technology, an International Journal*, 19, 1919-1928.

Mohamed, R. A. and Abo-Dahab, S. M. (2009). Influence of chemical reaction and thermal radiation on the heat and mass transfer in MHD micropolar flow over a vertical moving porous plate in a porous medium with heat generation. *International Journal of Thermal Sciences*, 48, 1800-1813.

Mohapatra, R., Pattanayak, H. and Mishra, S. R. (2015). Effect of chemical reaction on MHD micropolar fluid on a vertical surface through porous media with heat source. *International Journal of Innovative Research in Science, Engineering and Technology, 4*(9).

Olajuwon, B. I., Oahimire, J. I. and Waheed, M. A. (2014). Convection heat and mass transfer in a hydromagnetic flow of a micropolar fluid over a porous medium. *Theoret.Appl.Mech., 41*(2), 93-117.

Olanrewaju, P. O., Adeniyan, A. and Alao, S. F. (2013). Soret and Dufour effects on hydromagnetic free convection flow with heat and mass transfer past a porous plate in the presence of chemical reaction and thermal radiation. *Far East Journal of Applied Mathematics, 80*(1), 41-66.

Parida, S. K., Panda, S and Rout, B. R. (2015). MHD boundary layer slip flow and radiative nonlinear heat transfer over a flat plate with variable fluid properties and thermophoresis. *Alexandria Engineering Journal, 54*, 941-953.

Pal, D. and Chatterjee, S. (2010). Heat and mass transfer in MHD non-Darcian flow of a micropolar fluid over a stretching sheet embedded in a porous media with non-uniform heat source and thermal radiation. *Commun Nonlinear Sci. Numer Simulat, 15*, 1843-1857.

Pal, D. and Mondal, H. (20141). Effect of Soret Dufour, chemical reaction and thermal radiation on MHD non-Darcy unsteady mixed convective heat and mass transfer over a stretching sheet. *Commun Nonlinear Sci Numer Simulat, 16*, 1942-1958. doi:10.1016/j.cnsns.2010.08.033

Peddieson, J. (1972). An application of the micropolar model to the calculation of a turbulent shear flow. *Int. J. Eng. Sci., 10*, 23-32.

Rahman, M. M. and Sultana, T. (2008). Radiative Heat transfer flow of micropolar fluid with variable heat flux in a porous medium. *Nonlinear Analysis modelling and Control, 13*(1), 71-87.

Qasim, M., Khan, I. and Shafle, S. (2013). Heat transfer in a micropolar fluid over a stretching sheet with Newtonian heating. *Plos One, 8*(4), 1-6.

Rahman, M. M., Aziz, A. and Al-Lawatia, M. A. (2010). Heat transfer in micropolar fluid along an inclined permeable plate with variable fluid properties, *Int. J of Thermal Sciences*, 49, 993-1002.

Reddy, G. V. R. and Chamkha, A. J. (2014). Lie group analysis of chemical reaction effects on MHD free convection dissipative fluid flow past an inclined porous surface. *Int. J. of Numerical Methods for Heat and Fluid Flow, 25*, 1557-1573.

Reena and Rana, U. S. (2009). Effect of Dust Particles on rotating micropolar fluid heated from below saturating a porous medium. *Applications and Applied Mathematics: An International Journal, 4*, 189-217.

Salawu, S. O. and Fatunmbi, E. O. (2017). Dissipative heat transfer of micropolar hydromagnetic variable electric conductivity fluid past inclined plate with Joule heating and non-uniform heat generation, *Asian Journal of Physical and Chemical Sciences, 2*(1), 1-10.

Srinivasacharya, D. and Mendu, U. (2014). Free convection in MHD micropolar fluid with radiation and chemical reaction effects. *Chem. Ind. Chem. Eng. 20,*(2), 183-195.

Talbot, L., Cheng R. K., Scheffer, R. W. and Wills, D. P. (1980). Thermophoresis of particles in a heated boundary layer. *J Fluid Mech, 101*, 737–58.